# Pairing versus quarteting coherence length

D.S. Delion <sup>1,2,3</sup> and V.V. Baran <sup>1,4</sup>

<sup>1</sup> "Horia Hulubei" National Institute of Physics and Nuclear Engineering,
30 Reactorului, POB MG-6, RO-077125, Bucharest-Măgurele, România

<sup>2</sup> Academy of Romanian Scientists, 54 Splaiul Independenței RO-050085, Bucharest, România

<sup>3</sup> Bioterra University, 81 Gârlei RO-013724, Bucharest, România

<sup>4</sup> Department of Physics, University of Bucharest, 405 Atomiştilor,
POB MG-11, RO-077125, Bucharest-Măgurele, România

(Dated: August 10, 2018)

We systematically analyze the coherence length in even-even nuclei. The pairing coherence length in the spin-singlet channel for the effective density dependent delta (DDD) and Gaussian interaction is estimated. We consider in our calculations bound states as well as narrow resonances. It turns out that the pairing gaps given by the DDD interaction are similar to those of the Gaussian potential if one renormalizes the radial width to the nuclear radius. The correlations induced by the pairing interaction have in all considered cases a long range character inside the nucleus and decrease towards the surface. The mean coherence length is larger than the geometrical radius for light nuclei and approaches this value for heavy nuclei. The effect of the temperature and states in continuum is investigated. Strong shell effects are evidenced, especially for protons. We generalize this concept to quartets by considering similar relations, but between proton and neutron pairs. The quartet coherence length has a similar shape, but with larger values on the nuclear surface. We evidence the important role of proton-neutron correlations by estimating the so-called alpha coherence length. which takes into account the overlap with the proton-neutron part of the  $\alpha$ -particle wave function. It turns out that it does not depend on the nuclear size and has a value comparable to the free  $\alpha$ particle radius. We have shown that pairing correlations are mainly concentrated inside the nucleus, while quarteting correlations are connected to the nuclear surface.

PACS numbers: 21.30.Fe, 24.10.Cn, 25.70.Ef Keywords: Coherence length, Density-dependent pairing potential, Gaussian pairing potential, Pairing correlations, Quarteting correlations

#### I. INTRODUCTION

The concept of coherence has a general character being connected to the linear superposition of quantum states. Two-body coherence properties in nuclear structure are directly connected to the properties of low-lying collective states. Collective excitations are microscopically described by a superposition of creation pair operators acting on the ground state, described by a coherent state within the Random Phase Approximation (RPA). The coherent state in this context is defined as an exponential excitation of products between pair operators acting on the vacuum state [1]. It is well known that ground state properties of even-even nuclei are well reproduced by the pairing interaction [2–4]. The wave function within the Bardeen-Cooper-Schrieffer (BCS) pairing approach is also of a coherent type, i.e. an exponential excitation of the pair creation operators acting on the vacuum state.

The spatial distribution of the two-particle density is very important in understanding nuclear correlations [5, 6]. In particular, in Ref. [7] it was analyzed the relation between coherence and chaotic properties of the nuclear pairing. The coherence property is characterized by the so-called coherence length, defined as the root mean square distance averaged over the density. For superfluid nuclei this average is usually performed over the pairing density. In Refs. [8–10] it was shown that this quantity is relatively large, comparable to the nuclear size inside the

nucleus and decreases beyond the nuclear surface. This picture of an extended di-nuclear cluster can be understood in terms of the Pauli blocking, hindering nucleons to cluster together inside the nucleus and, therefore, the cluster loses binding and becomes larger. It is in contrast to the  $\alpha$ -clustering phenomenon, which takes place in a narrow region close to the surface area [11, 12], being connected to the very large binding energy of an  $\alpha$ -particle moving in a low density region [13]. Thus, we expect that the corresponding correlation length estimated between proton and neutron pairs will have significantly smaller value.

The finiteness of nuclear systems also has important consequences as far as thermal properties are concerned. Pairing correlations in finite nuclei do not vanish at some critical temperature, but they slowly decrease over several MeV [14, 15]. This can be theoretically obtained by projecting the particle number in the BCS theory [16]. However, hints about such behaviour can be extracted in the unprojected BCS approach from the spatial properties of the correlations.

In this paper we will perform a systematic analysis of the pairing coherence length and a comparison to the similar quantity defined for quartets. In Section II we give the necessary theoretical background concerning pairing equations containing resonant states and coherence length. In Section III we perform a systematic analysis of the coherence length and in the last Section we draw Conclusions.

### II. THEORETICAL BACKGROUND

#### II.1. Pairing equations

In order to investigate two-body correlations we expand the wave function of N+2 particles in terms of the wave function of N particles as follows

$$|\Psi_{N+2}\rangle = \hat{\kappa}|\Psi_{N}\rangle = \sum_{\epsilon} X_{\epsilon} \left[\hat{a}_{\epsilon}^{\dagger} \otimes \hat{a}_{\epsilon}^{\dagger}\right]_{0} |\Psi_{N}\rangle . \quad (2.1)$$

We will consider in our calculations the spherical approximation. Thus, the operator  $\hat{a}_{\epsilon}^{\dagger}$  creates a single particle (sp) eigenstate of the spherical mean field potential with standard quantum numbers  $\epsilon \equiv (\epsilon lj)$ . In the configuration representation one has

$$\langle \mathbf{r}, \mathbf{s} | \hat{a}_{\epsilon m}^{\dagger} | 0 \rangle \equiv \psi_{\epsilon m}(\mathbf{r}, \mathbf{s}) = \left[ \varphi_{\epsilon}(\mathbf{r}) \otimes \chi_{\frac{1}{2}}(\mathbf{s}) \right]_{jm}$$
$$\varphi_{\epsilon \mu}(\mathbf{r}) = \varphi_{\epsilon}(r) i^{l} Y_{l\mu}(\hat{r}) \equiv \frac{f_{\epsilon}(r)}{r} i^{l} Y_{l\mu}(\hat{r}) , \quad (2.2)$$

where  $\varphi_{\epsilon}(r)$  is the radial wave function and the rest of the notation is standard.

The operator  $\hat{\kappa}$  in Eq. (2.1) is called within the decay theory two-particle formation amplitude. In the absence of two-body correlations, when the wave functions are Slater determinants, this relation is nothing else than the Laplace expansion of the  $(N+2)\times(N+2)$  normalized determinant in terms of  $N\times N$  times  $2\times 2$  normalized determinants.

The most important two-body correlation beyond the mean field in even-even nuclei is given by the pairing interaction. We will describe such systems within the standard BCS approach, where the averaged particle number is conserved, separately for protons and neutrons. Thus, both wave functions in Eq. (2.1) have a BCS ansatz and

the operator  $\hat{\kappa}$ , connecting N+2 with N systems, is called pairing density operator. In this case the expansion coefficient

$$X_{\epsilon} = \frac{1}{2} \langle BCS_{N+2} | \left[ \hat{a}_{\epsilon}^{\dagger} \otimes \hat{a}_{\epsilon}^{\dagger} \right]_{0} | BCS_{N} \rangle$$
$$= \frac{\sqrt{2j+1}}{2} x_{\epsilon} , \qquad (2.3)$$

is given in terms of BCS amplitudes as follows

$$\begin{split} x_{\epsilon} &\equiv u_{\epsilon}^{(N+2)} v_{\epsilon}^{(N)} \prod_{k \neq \epsilon} \left[ u_{k}^{(N+2)} u_{k}^{(N)} + v_{k}^{(N+2)} v_{k}^{(N)} \right] \\ &\approx u_{\epsilon}^{(N)} v_{\epsilon}^{(N)} \approx u_{\epsilon}^{(N+2)} v_{\epsilon}^{(N+2)} \ . \end{split} \tag{2.4}$$

We will consider in our basis bound sp states with negative energy, as well as relatively narrow sp resonances with positive energy. Relatively narrow resonances are similar to bound states and can be normalized to unity in the internal region, but at large distances they behave like outgoing waves

$$\varphi_{\epsilon}(r) \to_{r \to \infty} M_{\epsilon} \frac{H_l^{(+)}(r)}{r} \equiv M_{\epsilon} \frac{G_l(r) + iF_l(r)}{r} , (2.5)$$

in terms of spherical Hankel functions for neutrons and Coulomb-Hankel functions for protons. The coefficients  $M_{\epsilon}$  are called scattering amplitudes and their squared values are proportional to sp partial decay widths.

The states in continuum play an important role on pairing correlations, especially for nuclei close to the drip lines [6, 17–21]. For nuclear structure calculations the background contribution is not relevant and only relatively narrow resonant states are important [22, 23]. A very good approximation for BCS calculations is to neglect the finite resonance width, i.e. to treat the resonances as bound-like states [24]. We label bound states by a and resonances with positive energy by r. We treat proton and neutron pairing separately; for a given isospin index the generalized system of BCS equations for gap parameters  $\Delta_a$ ,  $\Delta_r$  and number of particles N is

$$\Delta_{a} = \sum_{a'} \left( j_{a'} + \frac{1}{2} \right) V_{a,a'} \frac{\Delta_{a'}}{2\sqrt{(\epsilon_{a'} - \lambda)^{2} + \Delta_{a'}^{2}}} + \sum_{r} \left( j_{r} + \frac{1}{2} \right) V_{a,r} \frac{\Delta_{r}}{2\sqrt{(\epsilon_{r} - \lambda)^{2} + \Delta_{r}^{2}}} ,$$

$$\Delta_{r} = \sum_{a'} \left( j_{a'} + \frac{1}{2} \right) V_{r,a'} \frac{\Delta_{a'}}{2\sqrt{(\epsilon_{a'} - \lambda)^{2} + \Delta_{a'}^{2}}} + \sum_{r'} \left( j_{r'} + \frac{1}{2} \right) V_{r,r'} \frac{\Delta_{r'}}{2\sqrt{(\epsilon_{r'} - \lambda)^{2} + \Delta_{r'}^{2}}} ,$$

$$N = \sum_{a} \left( j_{a} + \frac{1}{2} \right) \left( 1 - \frac{\epsilon_{a} - \lambda}{\sqrt{(\epsilon_{a} - \lambda)^{2} + \Delta_{a}^{2}}} \right) + \sum_{r} (j_{r} + \frac{1}{2}) \left( 1 - \frac{\epsilon_{r} - \lambda}{\sqrt{(\epsilon_{r} - \lambda)^{2} + \Delta_{r}^{2}}} \right) ,$$
(2.6)

where  $\lambda$  is the chemical potential and the potential matrix elements  $V_{\alpha,\beta}$  are computed according to Eq. (2.6) of [25].

We will investigate pairing in excited nuclei by using the temperature-dependent equations with anomalous and normal densities, respectively

$$\langle a_{\epsilon} a_{\bar{\epsilon}} \rangle = u_{\epsilon} v_{\epsilon} \tanh \frac{\beta E_{\epsilon}}{2}$$
  
 $\langle a_{\epsilon}^{\dagger} a_{\epsilon} \rangle = v_{\epsilon}^{2} + (u_{\epsilon}^{2} - v_{\epsilon}^{2})/(e^{\beta E_{\epsilon}} + 1)$ . (2.7)

### II.2. Pairing coherence length

The two-body operator entering the pairing density (2.1) can be written in the configuration representation. By using the recoupling from j-j to the L-S scheme, one obtains spin-singlet and spin-triplet components. Our calculations have shown that the largest contribution is given by the spin-singlet component, given the following expression

$$\kappa(\mathbf{r}_{1}, \mathbf{r}_{2}) = \sum_{\epsilon} z_{\epsilon} \left[ \varphi_{\epsilon}(\mathbf{r}_{1}) \otimes \varphi_{\epsilon}(\mathbf{r}_{2}) \right]_{0}$$
$$= \sum_{\epsilon} z_{\epsilon} \frac{f_{\epsilon}(r_{1}) f_{\epsilon}(r_{2})}{r_{1} r_{2}} \mathcal{Y}_{l}(\cos \theta) , \qquad (2.8)$$

in terms of two-particle azimuthal harmonics

$$\mathcal{Y}_{l}(\cos \theta) = \left[i^{l}Y_{l}(\hat{r}_{1}) \otimes i^{l}Y_{l}(\hat{r}_{2})\right]_{0}$$

$$= \frac{\sqrt{2l+1}}{4\pi} P_{l}(\cos \theta) , \qquad (2.9)$$

where  $\theta$  is the angle between particle radii and the expansion coefficient is given by

$$z_{\epsilon} = x_{\epsilon} \sqrt{j + \frac{1}{2}} \langle (ll)0, \left(\frac{1}{2}\frac{1}{2}\right) 0; 0 | \left(l\frac{1}{2}\right) j, \left(l\frac{1}{2}\right) j; 0 \rangle ,$$

$$(2.10)$$

in terms of LS-jj recoupling brackets. By expanding the sp wave function with respect to the harmonic oscillator (ho) basis

$$\varphi_{\epsilon\mu}(\mathbf{r}) = \sum_{n} c_{n\epsilon} \phi_{nl\mu}^{(\beta)}(\mathbf{r})$$
$$\phi_{nl\mu}^{(\beta)}(\mathbf{r}) = \phi_{nl}^{(\beta)}(r) i^{l} Y_{l\mu}(\hat{r}) , \qquad (2.11)$$

where  $\beta = M_N \omega / \hbar$  is the standard ho parameter, and by using the Talmi-Moshinski transformation to relative  $\mathbf{r} = \mathbf{r_1} - \mathbf{r_2}$  and center of mass (c.o.m.) coordinate  $\mathbf{R} = (\mathbf{r_1} + \mathbf{r_2})/2$  one obtains the following expansion

$$\kappa(r, R, \theta) = \sum_{\lambda} f_{\lambda}(r, R) \mathcal{Y}_{\lambda}(\cos \theta) ,$$
 (2.12)

with expansion coefficients given by

$$f_{\lambda}(r,R) = \sum_{nN} \mathcal{G}_{nN\lambda} \phi_{n\lambda}^{(\beta/2)}(r) \ \Phi_{N\lambda}^{(2\beta)}(R) \ , \quad (2.13)$$

where

$$\mathcal{G}_{nN\lambda} \equiv \sum_{\epsilon} z_{\epsilon} \sum_{n_1 n_2} c_{n_1 \epsilon} c_{n_2 \epsilon} \langle n \lambda N \lambda; 0 | n_1 l n_2 l; 0 \rangle \ . \tag{2.14}$$

Here, the bracket denotes the standard Talmi-Moshinsky recoupling coefficient. By averaging over the angle  $\theta$  we get

$$\bar{\kappa}^{2}(r,R) = \frac{1}{2} \int_{-1}^{1} \kappa^{2}(r,R,\theta) d\cos\theta$$
$$= \frac{1}{(4\pi)^{2}} \sum_{\lambda} f_{\lambda}^{2}(r,R) . \qquad (2.15)$$

The coherence length is defined as follows

$$\xi(R) = \sqrt{\frac{I^{(2)}(R)}{I^{(1)}(R)}}$$

$$\equiv \sqrt{\int_0^\infty dr \ r^2 \ w(r,R)} \ , \tag{2.16}$$

in terms of the integrals

$$I^{(p)}(R) \equiv \int_0^\infty dr \ r^{2p} \ \bar{\kappa}^2(r,R)$$

$$= \sum_{\lambda N N'} \Phi_{N\lambda}^{(2\beta)}(R) \Phi_{N'\lambda}^{(2\beta)}(R)$$

$$\times \sum_{nn'} \mathcal{G}_{nN\lambda} \mathcal{G}_{n'N'\lambda} \int_0^\infty dr \ r^{2p} \phi_{n\lambda}^{(\beta/2)}(r) \phi_{n'\lambda}^{(\beta/2)}(r) \ . \tag{2.17}$$

Let us finally mention that the quantity  $x_{\epsilon}$ , defined by Eq. (2.4), is also called "anomalous" density, while the quantity

$$y_{\epsilon} = v_{\epsilon}^2 \ . \tag{2.18}$$

is called "normal" density. Therefore  $\kappa$ , defined by Eq. (2.8), can be called "anomalous" coherence length, while a similar quantity  $\kappa_0$  defined by using the "normal" density is called "normal" coherence length.

### II.3. Quarteting correlations

We will investigate quarteting correlations in medium and heavy  $\alpha$ -decaying nuclei, where the valence protons and neutrons occupy different major shells. The standard assumption to build a quartet from two protons and two neutrons in such nuclei is to consider proton and neutron pairing separately [26, 27]. Therefore the system of  $N_{\pi}$  + 2,  $N_{\nu}$  + 2 nucleons can be expressed in terms of  $N_{\pi}$ ,  $N_{\nu}$  nucleons in a factorized way as follows

$$|\Psi_{N_-+2,N_++2}\rangle = \hat{\kappa}_{\pi}\hat{\kappa}_{\nu}|\Psi_{N_-N_+}\rangle , \qquad (2.19)$$

where  $\kappa_{\tau}$  is defined by Eq. (2.1). Thus, the quartet wave function is a product between proton and neutron two-body wave functions (2.12). Anyway, calculations in infinite nuclear matter suggest that  $\alpha$ -clusters can occur only at relative small nuclear densities compared to the equilibrium value and the proton-neutron correlations play an important role [13]. Thus, an  $\alpha$ -particle can be formed only in the surface region where the nuclear density diminishes and proton-neutron correlations become relevant. This situation can be simulated by a proper modification of the single particle mean field by adding a gaussian interaction in the surface region [28] and still by keeping the factorized ansatz (2.19). This can expain why an  $\alpha$ -particle can be formed from two protons and two neutrons lying in different major shells. This additional ansatz of the single particle mean field

was recently confirmed by microscopic calculations [29] and fission-like theory [30]. Anyway, this modification is important in order to reproduce the absolute value of the half-life, but has a minor influence on the coherence length.

In order to describe quartets we introduce the relative and c.o.m. coordinates for proton, neutron and protonneutron systems, respectively:

$$\mathbf{r}_{\pi} = \mathbf{r}_{1} - \mathbf{r}_{2} , \quad \mathbf{R}_{\pi} = \frac{\mathbf{r}_{1} + \mathbf{r}_{2}}{2}$$

$$\mathbf{r}_{\nu} = \mathbf{r}_{3} - \mathbf{r}_{4} , \quad \mathbf{R}_{\nu} = \frac{\mathbf{r}_{3} + \mathbf{r}_{4}}{2}$$

$$\mathbf{r}_{\alpha} = \mathbf{R}_{\pi} - \mathbf{R}_{\nu} , \quad \mathbf{R}_{\alpha} = \frac{\mathbf{R}_{\pi} + \mathbf{R}_{\nu}}{2} , \quad (2.20)$$

where we labeled by 1, 2 proton and by 3, 4 neutron coordinates. The internal  $\alpha$ -particle wave function is given by the product between the lowest proton, neutron and proton-neutron ho orbitals

$$\psi_{\alpha} = \phi_{00}^{(\beta_{\alpha}/2)}(r_{\pi})\phi_{00}^{(\beta_{\alpha}/2)}(r_{\nu})\phi_{00}^{(\beta_{\alpha})}(r_{\alpha}) , \quad (2.21)$$

where  $\beta_{\alpha} \approx 0.5 \ fm^{-2}$  is the free  $\alpha$ -particle ho parameter measured by electron scattering experiments [26]. This parameter is about 2-3 times larger than the similar sp ho parameter in heavy  $\alpha$ -emitters, due to the fact that  $\alpha$ -particle is a very bound object.

We will describe quarteting correlations between proton and neutron pairs by overlapping the relative coordinates to the corresponding components of the  $\alpha$ -particle wave function (2.21). We will proceed in two steps.

### A. Quarteting correlation length

Let us first consider only the overlap with respect to proton and neutron relative coordinates  $r_{\pi}$ ,  $r_{\nu}$ , by keeping free the internal proton-neutron coordinate  $r_{\alpha}$ . Thus, we consider independent from each other proton and neutron pairs by neglecting proton-neutron correlations. Therefore we can define the quarteting density in analogy to the pairing density, but between the proton and neutron pairs (instead of fermions):

$$\kappa_{q}(\mathbf{R}_{\pi}, \mathbf{R}_{\nu}) = \langle \kappa_{\pi}(\mathbf{r}_{1}, \mathbf{r}_{2}) | \phi_{00}^{(\beta_{\alpha}/2)}(r_{\pi}) \rangle \times \langle \kappa_{\nu}(\mathbf{r}_{3}, \mathbf{r}_{4}) | \phi_{00}^{(\beta_{\alpha}/2)}(r_{\nu}) \rangle . \quad (2.22)$$

By recoupling the product between proton and neutron pairs (2.12) to the relative and c.o.m. pair coordinates one obtains for the leading monopole component the following relation

$$\kappa_{q}(r_{\alpha}, R_{\alpha}) \approx \kappa_{q}^{(0)}(r_{\alpha}, R_{\alpha}) = \sum_{N_{\pi}, N_{\nu}} G_{\pi}(N_{\pi}) G_{\nu}(N_{\nu})$$

$$\times \sum_{n_{\alpha}} \langle n_{\alpha} 0 N_{\alpha} 0; 0 | N_{\pi} 0 N_{\nu} 0; 0 \rangle \phi_{n_{\alpha} 0}^{(\beta)}(r_{\alpha}) \phi_{N_{\alpha} 0}^{(4\beta)}(R_{\alpha}) ,$$

$$(2.23)$$

in terms of Moshinsky brackets and the proton/neutron monopole G-coefficients (2.14)

$$G_{\tau}(N_{\tau}) = \sum_{n_{\tau}} \mathcal{G}_{n_{\tau}N_{\tau}0} \langle \phi_{n_{\tau}0}^{(\beta/2)}(r_{\tau}) | \phi_{00}^{(\beta_{\alpha}/2)}(r_{\tau}) \rangle$$
$$\tau = \pi, \nu . \qquad (2.24)$$

It does not depend on angles and therefore one can define the quarteting coherence length  $\xi_q(R_\alpha)$  without any additional angular average (2.15) by using in Eqs. (2.16) and (2.17) the quarteting density squared  $\kappa_q^2(r_\alpha, R_\alpha)$ .

# B. Alpha coherence length

The next step is to consider proton-neutron correlations. They are described by the corresponding part in the  $\alpha$ -particle wave function (2.21) given by  $\phi_{00}^{(\beta_{\alpha})}(r_{\alpha})$ . In order to account for the narrow proton-neutron spatial distribution in the free  $\alpha$ -particle one defines the so-called alpha coherence length  $\xi_{\alpha}(R_{\alpha})$  by using the alpha density

$$\kappa_{\alpha}(r_{\alpha}, R_{\alpha}) = \kappa_{q}(r_{\alpha}, R_{\alpha})\phi_{00}^{(\beta_{\alpha})}(r_{\alpha}) , \qquad (2.25)$$

in performing the integrals (2.17).

Let us finally mention that the integral of the alpha density over the relative proton-neutron coordinate

$$\mathcal{F}(R_{\alpha}) = \int_{0}^{\infty} \kappa_{\alpha}(r_{\alpha}, R_{\alpha}) r_{\alpha}^{2} dr_{\alpha} , \qquad (2.26)$$

defines the formation amplitude and its square describes the probability to find an  $\alpha$ -particle in the quartet wave function [12, 26].

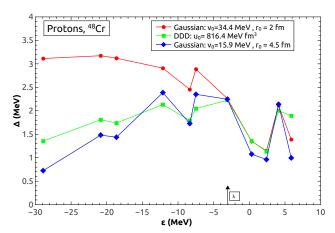


FIG. 1. Paring gap defined by the first two lines of Eq. (2.6) versus  $\epsilon$  in <sup>48</sup>Cr for DDD potential (squares) and Gaussian potentials with  $r_0 = 2$  fm (circles) and  $r_0 = R_N$  (diamonds).

# III. NUMERICAL APPLICATION

We analyzed all even-even nuclei with 20 < Z < 100 and known experimental pairing gaps, determined by the binding energies of neighbouring nuclei [31].

TABLE I. Proton quantum numbers, sp spectrum, decay widths and gap parameters for the Gaussian, renormalized Gaussian and DDD interactions in <sup>48</sup>Cr, given by the diagonalization of the Woods-Saxon mean field with universal parametrisation [32].

No.	l	2j	$\epsilon \; ({\rm MeV})$	$\Gamma \; ({\rm MeV})$	$\Delta_{2\mathrm{fm}}(\mathrm{MeV})$	$\Delta_{4.5 \mathrm{fm}} (\mathrm{MeV})$	$\Delta_{\rm DDD}({\rm MeV})$
1	0	1	-28.911	-	3.114	1.354	0.724
2	1	3	-20.837	-	3.173	1.810	1.482
3	1	1	-18.638	-	3.121	1.739	1.436
4	2	5	-12.118	-	2.908	2.131	2.387
5	0	1	-8.349	-	2.454	1.795	1.728
6	2	3	-7.488	-	2.886	2.047	2.351
7	3	7	-3.079	-	.261	2.224	2.246
8	1	3	0.322	0.000	1.349	1.356	1.076
9	1	1	2.403	0.046	1.149	1.133	0.962
10	3	5	4.101	0.024	2.114	2.003	2.139
11	4	9	5.874	0.055	1.389	1.893	0.996

For the nuclear mean field we used a standard Woods-Saxon potential with universal parametrization [32]. We considered in our sp basis all bound states and resonances in continuum up to  $e_{max}=10$  MeV with a sp decay width  $\Gamma \leq 1$  MeV. As an example we give in Table I the proton sp spectrum for <sup>48</sup>Cr. Here, there are given level number, angular momentum, twice the total spin, sp energy, decay width of sp states in continuum and pairing gaps for the interactions considered below.

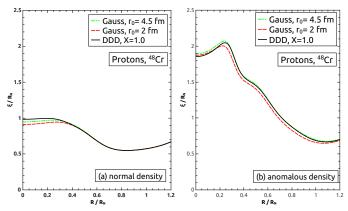


FIG. 2. Proton coherence length divided by geometrical radius versus c.o.m. radius in  $^{48}$ Cr computed with "normal" (a) and "anomalous" densities (b) for DDD potential (solid line) and Gaussian potentials with  $r_0$ = 2 fm (long dashes) and  $r_0 = R_N$  (short dashes).

We solved the BCS equations (2.6) separately for protons and neutrons with two widely used types of nucleon-nucleon pairing interactions:

#### I. Gaussian interaction

It is defined by the following ansatz:

$$v(r_{12}) = -v_0 e^{-[r_{12}/r_0]^2}$$
, (3.1)

depending on the relative radius  $r_{12}$ . Here, the width parameter  $r_0=2$  fm corresponds to the spin-singlet "bare" value in the free space. The corresponding value of the effective potential strength  $v_0$  is determined by the gap parameter at the Fermi level, which should be equal to the experimental value.

# II. Density dependent delta (DDD) interaction

It is known that the strength of the effective pairing interaction depends upon the local density [17, 18], given by the following phenomenological ansatz [19]

$$v(\mathbf{r}, \mathbf{r}') = u_0 \delta(\mathbf{r} - \mathbf{r}') \left\{ 1 - X \left[ \frac{\rho_N(\mathbf{r})}{\rho_N^{(0)}} \right]^{\gamma} \right\} , \quad (3.2)$$

in terms of the nuclear density  $\rho_N$ . The value X=1 corresponds to the surface DDD interaction.

As an example, in Fig. 1 we plotted the pairing gap (2.6) versus sp energy for  $^{48}$ Cr, given in Table I. Here, circles correspond to the Gaussian interaction in the free space with  $r_0=2$  fm. Notice large values for states below the Fermi level. The gaps given by DDD interaction with  $X = \gamma=1$  are plotted by squares and the values below the Fermi level are significantly smaller that the Fermi gap.

It is interesting to point out that a very similar behaviour has the Gaussian interaction where the width parameter is renormalized to the geometrical nuclear radius (in fm)  $r_0 = R_N = 1.2A^{1/3}$ . A di-nuclear cluster inside nuclear matter has different properties with respect to the free space. It considerably loses the binding

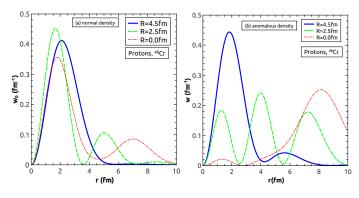


FIG. 3. The integrand of the proton coherence length versus the relative radius radius in  $^{48}$ Cr, computed with "normal" (a) and "anomalous" densities (b) for different c.o.m. radii. Here, we used the Gaussian interaction withn  $r_0=2$  fm.

property due to the Pauli blocking, becoming larger and therefore the effective pairing interaction has a more extended shape. Above the Fermi sea we obtained similar values in all cases.

In Fig. 2 (a) we plotted the proton coherence length given by Eq. (2.16) divided by the nuclear radius  $R_N$ , as a function of the ratio between c.o.m. and nuclear radius  $R/R_N$  in <sup>48</sup>Cr. Here we used the "normal" density while in Fig. 2 (b) we used the "anomalous" density. Notice that that all cases, plotted by different symbols explained in caption, have very similar shapes. Thus, the coherence length is not sensitive to the radial shape of the interaction. The "normal" coherence length is equal to the nuclear radius in the internal region and diminishes by a factor 0.5 on the surface. The "anomalous" coherence length has a similar shape, but with twice larger internal value. This picture is very different from the dependence of the two-body wave function versus c.o.m. radius, which is peaked on the nuclear surface [25].

In order to better understand the behaviour of the coherence length we plotted in Fig. 3 (a) the integrand of the "normal" correlation length  $w_0(r,R)$ , given by the second line of Eq. (2.16), versus the relative radius r for three values of the c.o.m. radius R=4.5 fm (solid line), 2 fm (long dashes) and 0 fm (short dashes). Here, we used the "bare" version of the Gaussian interaction. Notice that the three curves have a similar shape, strongly peaked around 2 fm. We obtain completely different plots for the integrand of the "anomalous" coherence length w(r,R). They are given in Fig. 3 (b). The distribution corresponding to the c.o.m. radius on surface R=4.5 fm (solid line) is peaked around the free singlet value of the Gaussian width i.e. r=2 fm. On the contrary, the distribution corresponding to a smaller radius R=2.5 (long dashes) is peaked around a much larger value r=7 fm.

Our conclusions are in agreement with Ref. [8], where in Fig. 5 the "anomalous" coherence length of the pairing interaction was estimated within the more sophisticated Hartree-Fock-Bogoljubov (HFB) approach, by using the

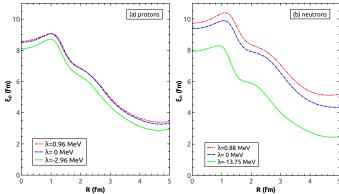


FIG. 4. (a) Proton coherence length versus c.o.m. radius for different chemical potentials  $\lambda$ =-2.96 MeV (solid line), 0 MeV (long dashes) and 0.96 MeV (short dashes) in  $^{48}{\rm Cr}$ . (b) Neutron coherence length versus c.o.m. radius for different chemical potentials  $\lambda$ =-13.75 MeV (solid line), 0 MeV (long dashes) and 0.88 MeV (short dashes) in  $^{48}{\rm Cr}$ .

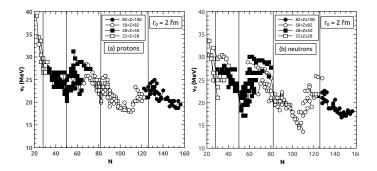


FIG. 5. Strength parameter of the Gaussian interaction, corresponding to  $r_0=2$  fm, versus neutron number for proton (a) and neutron systems (b).

Gogny force for Ni isotopes. The shape is similar, predicting a mean coherence length of about 6 fm in the internal region and decreasing as one approaches the nuclear surface and reaching the value of 2 fm just outside the nucleus.

Most of the exotic nuclei close to the drip lines have the last nucleon in continuum. Therefore we investigated the dependence of the coherence length on the Fermi level, by changing the real part of the Woods-Saxon potential. We plotted in Fig. 4 (a) the proton coherence length versus c.o.m. radius in <sup>48</sup>Cr, for different values of the chemical potential. One sees that it increases by increasing the chemical potential. This effect is stronger for neutrons, as seen in Fig. 4 (b), due to the absence of the Coulomb barrier. Therefore, in exotic nuclei close to drip lines the nucleons become more correlated.

Then we performed a systematic analysis of the "anomalous" coherence length (by simply calling it coherence length) for even-even nuclei with 20 < Z < 100.

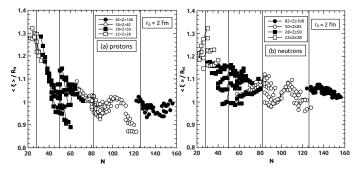


FIG. 6. Ratio  $\langle \xi \rangle / R_N$ , corresponding to a Gaussian interaction with  $r_0$ =2 fm, versus neutron number for proton (a) and neutron systems (b).

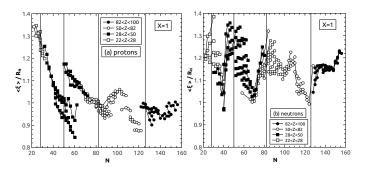


FIG. 7. Ratio  $\langle \xi \rangle / R_N$ , corresponding to the DDD interaction (3.2) with  $X = \gamma = 1$ , versus neutron number for proton (a) and neutron systems (b).

In Fig. 5 (a) we plotted the effective strength  $v_0$  as a function of the neutron number for protons corresponding to Gaussian interaction with  $r_0=2$  fm. The isotope chains are connected by solid lines and magic numbers are indicated by vertical lines. Different regions are plotted by open squares (20 < Z < 28), filled squares (28 < Z < 50), open circles (50 < Z < 82) and filled circles (82 < Z < 100). As a general trend we remark a strong decreasing behaviour with the increase of the neutron number. We notice a remarkable feature, namely it has almost the singlet "bare" value in the free space  $v_0 \sim$ 35 MeV for very light nuclei. The strength strongly decreases up to  $v_0 \sim 20$  MeV for heavy nuclei, except the regions around magic numbers. In Fig. 5 (b) we give a similar plot for neutrons. Notice that in this case shell effects are stronger.

In Fig. 6 (a) we analyzed the mean coherence length  $\langle \xi \rangle$  for protons, corresponding to the Gaussian interaction with the free value of the width parameter  $r_0{=}2$  fm as a function of neutrons. The ratio of this quantity to the nuclear radius decreases from 1.4 for light nuclei up to around unity for heavy nuclei. In Fig. 6 (b) we give similar results for neutrons. As a general trend, the coherence length is larger for neutrons due to the absence of the Coulomb barrier, but the shell effects are stronger

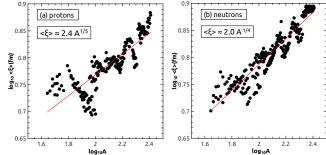


FIG. 8. Logarithm of the ratio  $\langle \xi \rangle / R_N$  versus logarithm of the mass number for protons (a) and neutrons (b).

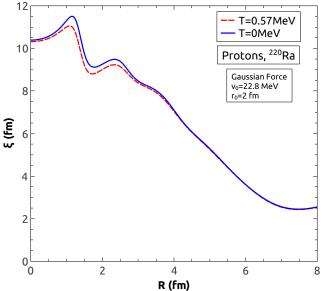


FIG. 9. Proton coherence length versus c.o.m. radius in  $^{220}$ Ra computed for T=0 (solid line), T=0.5675 MeV  $\lesssim T_c$  (long dashes), for a Gaussian potential with  $r_0$ = 2 fm.

for protons.

We then investigated the density dependent pairing interaction given by Eq. (3.2) with  $X = \gamma = 1$  in Fig. 7. It turns out that the ratio  $\langle \xi \rangle / R_N$  has similar gross features, but with more pronounced shell oscillations. The fact that the coherence length for neutrons is larger is confirmed. It is interesting to notice the linear correlation between  $log_{10}\langle \xi \rangle$  and  $log_{10}A$ , plotted in Fig. 8 for the Gaussian pairing interaction with  $r_0=2$  fm.

In order to investigate the behaviour of the coherence length for excited states, in Fig. 9 we analyzed the role of the temperature. Firstly, we give for  $^{220}$ Ra the coherence length versus the pair c.o.m. radius for T=0 and just below the 'critical' temperature  $T_c\approx 0.57$  MeV (here the gap decreases below  $10^{-3}$  MeV). The pairing coherence length shows very little change in shape up to  $T_c$ . The

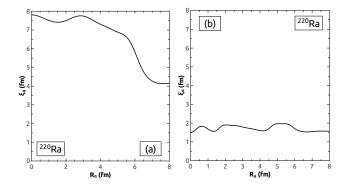
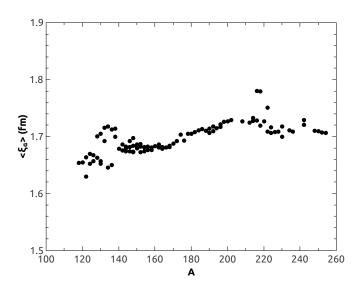


FIG. 10. (a) Quarteting coherence length in  $^{220}\mathrm{Ra}$  versus c.o.m. radius.

(b) Same as in (a) but for alpha coherence length.



 ${\it FIG.}$  11. Averaged alpha coherence length versus mass number.

strongest variation appears in the internal region, while on the surface, where the pairs are strongly coupled [8], there is indeed almost no change. As a measure of the pairing correlations, the coherence length would appear to indicate a gradual transition to the normal state with increasing temperature, as its behaviour is similar to that of the pairing gap in the particle number conserving case [16, 33].

Our purpose is to compare the pairing and quarteting coherence lengths. First we analyzed the quarteting coherence length, by using the quarteting density (2.22), for the  $\alpha$ -emitter  $^{220}\mathrm{Ra}$  as a function of c.o.m. radius in Fig. 10 (a). One notices a similar qualitative behaviour compared to the pairing coherence length, but the absolute values are larger on the nuclear surface. Our calculations have shown that the temperature practically does not change this dependence.

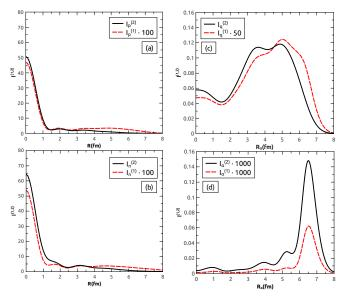


FIG. 12. The two terms  $I^{(p)}(R)$ , p=2 (solid line) p=1 (dashed line) given by Eq. (2.17), defining the pairing coherence length for protons (a), neutrons (b), quarteting coherence length (c) and alpha coherence length (d) versus the c.o.m. radius.

It turns out that the proton-neutron correlations, given by the overlap with the corresponding proton-neutron part of the  $\alpha$ -particle wave function (2.25), completely change this picture. One sees from Fig. 10 (b), where we plotted the alpha correlation length versus c.o.m. radius, that the values oscillate around the value of the geometrical radius of the  $\alpha$ -particle  $R_{\alpha}$ . Thus, our analysis confirm the crucial role played by proton-neutron correlations in the formation of the  $\alpha$ -particle. Finally, in Fig. 11 we plotted the mean value of the alpha coherence length for even-even  $\alpha$ -emitters above A=100. It has a quasi-constant value around 1.7 fm. Small local maxima correspond to regions above double magic nuclei  $^{132}$ Sn and  $^{208}$ Pb.

In order to better understand the difference between pairing and quarteting correlations we plotted in Fig. 12 the two terms  $I^{(p)}$ , p=2 (solid line) and p=1 (dashed line) given by Eq. (2.17) versus the c.o.m. radius. The two terms reach their maximal values for the pairing case (left panels) at R=0, while for the quarteting case (right panels) the maxima are centered around the surface region. The pairing coherence length for protons (a) and neutrons (b) is given by the ratio between solid and dashed curves which obviously decreases with increasing c.o.m. radius. Quarteting coherence length is given by the ratio between solid and dashed lines in Fig. 12 (c) which have slighly shifted broad maxima located below the nuclear surface. Although the two terms have completely different shapes compared to the pairing case, their ratio plotted in Fig. 10 (a) is also a decreasing function with respect to the c.o.m. radius.

The alpha coherence length, given by the ratio of the two curves in Fig. 12 (d), deserves special attention. These curves have very narrow maxima centered at the same point on the nuclear surface. Moreover, it turns out that the two curves are almost proportional and therefore their ratio leads to the quasiconstant value in Fig. 10 (b), close the  $\alpha$ -particle geometrical radius  $R_{\alpha}^{(0)}=1.2~4^{1/3}\approx 1.9~{\rm fm}$ . Notice that the shape of the curves in Fig. 12 (d), peaked on the nuclear surface, is similar to the standard  $\alpha$ -particle formation probability, given by the integral (2.26) squared [12, 28].

### IV. CONCLUSIONS

In conclusion, we have performed in this paper a systematic analysis of the pairing coherence length in the spin-singlet channel for various types of pairing interaction. We compared the DDD potential to the Gaussian interaction. We considered in our calculations bound states as well as narrow resonances.

As a very important conclusion we have shown that, by considering the singlet "bare" value of the width parameter  $r_0{=}2$  fm, the strength parameter reproducing the gap parameter for light nuclei is close to the singlet value in the free space  $v_0 \sim 35$  MeV and decreases up to  $v_0 \sim 20$  MeV for heavy nuclei. We have shown that the "renormalized" Gaussian interaction with a larger width parameter than its free value  $r_0{=}2$  fm (equal to the nuclear radius) has similar properties to the commonly used density dependent pairing potential.

It turns out that the pairing coherence length has similar properties for all considered interactions. It is larger than the geometrical radius for light nuclei and approaches this value for heavy nuclei. Our analysis evidenced strong shell effects.

The pairing coherence length slowly decreases with increasing temperature, indicating a gradual quenching of pairing correlations, as is natural in finite systems. In exotic nuclei close to drip lines, where the Fermi energy has positive values, the correlation length has larger values and therefore the spatial correlation increases.

The quarteting coherence length describes correlations between proton and neutron pairs, by overlapping their relative parts to the corresponding pp and nn components of the  $\alpha$ -particle wave function. It has a similar behaviour, but with larger values on the nuclear surface. We evidenced the important role played by protonneutron correlations by considering in addition the overlap with the pn component of the  $\alpha$ -particle wave function. They change completely the behaviour of the quarteting coherence length, namely the alpha correlation length has oscillating values around the  $\alpha$ -particle geometrical radius. Its mean value  $\approx 1.7$  fm weakly depends on the nuclear mass. The analysis of the two terms entering the definition of the coherence length reveales the main difference between the pairing and quarteting cases. It turns out that pairing correlations are larger inside nucleus, while quarteting correlations are connected to the nuclear surface.

### ACKNOWLEDGMENTS

This work has been supported by the project PN-II-ID-PCE-2011-3-0092 and NuPNET-SARFEN of the Romanian Ministry of Education and Research.

- [1] P. Ring and P. Schuck, *The Nuclear Many Body Problem* (Springer-Verlag, New York-Berlin, 1980).
- [2] D.J. Dean and M. Hjorth-Jensen, Rev. Mod. Phys. 75 607 (2003).
- [3] V. Zelevinsky and A. Volya, Nucl. Phys. A 731, 299 (2004).
- [4] S. Yoshida and H. Sagawa, Phys. Rev. C 77, 054308 (2008).
- [5] L. Ferreira, R.J. Liotta, C.H. Dasso, R.A. Broglia, and A. Winther, Nucl. Phys. A 426, 276 (1984).
- [6] K. Hagino and H. Sagawa, Phys. Rev. C 72, 044321 (2005).
- [7] A. Volya, V. Zelevinsky, and B.A. Brown, Phys. Rev. C 65, 054312 (2002).
- [8] N. Pillet, N. Sandulescu, and P. Schuck, Phys. Rev. C 76, 024310 (2007).
- [9] N. Pillet, N. Sandulescu, P. Schuck, and J.-F. Berger, Phys. Rev. C 81 034307 (2010).
- [10] X. Vinas, P. Schuck, and N. Pillet, Phys. Rev. C 82, 034314 (2010).
- [11] F.A. Janouch and R. J. Liotta, Phys. Rev. C 27, 896 (1983).

- [12] D.S. Delion *Theory of Particle and Cluster Emission*, (Springer-Verlag, New York-Berlin, 2010).
- [13] G. Ropke, A. Schnell, P. Schuck, and P. Nozieres, Phys. Rev. Lett. 80, 3177 (1998).
- [14] V. Zelevinsky, A. Volya, Phys. At. Nuclei 66 10 (2003).
- [15] A. Schiller  $\it et.~al.,$  Phys. Rev. C  $\bf 63$  021306R (2003).
- [16] T. Døssing et al., Phys. Rev. Lett. **75**, 1276 (1995).
- [17] G. Bertsch and H. Esbensen, Ann. Phys. (N.Y.) 209, 327 (1991).
- [18] P.J. Borycki, J. Dobaczewski, W. Nazarewicz, and M. V. Stoitsov, Phys. Rev. C 73, 044319 (2006).
- [19] J. Dobaczewski, W. Nazarewicz, T.R. Werner, J.F. Berger, C.R. Chinn, and J. Decharge, Phys. Rev. C 53, 2809 (1996).
- [20] M. Grasso, N. Sandulescu, N. Van Giai, and R. J. Liotta, Phys. Rev. C 64, 064321 (2001).
- [21] I. Hamamoto, Phys. Rev. C 73, 044317 (2006).
- [22] Id.R. Betan, G.G. Dussel, and R.J. Liotta, Phys. Rev. C 78, 044325 (2008).
- [23] Id.R. Betan, Nucl. Phys. A 879, (2012) 14 (2012).
- [24] D.S. Delion, D. Santos, P. Schuck, Phys. Lett. B 398, 1 (1997).

- [25] D.S. Delion, M. Baldo, and U. Lombardo, Nucl. Phys. A 593, 151 (1995).
- [26] H.J. Mang, Phys. Rev. 119, 1069 (1960).
- [27] A. Sandulescu, Nucl. Phys. A **37**, 332 (1962).
- [28] D.S. Delion and R.J. Liotta, Phys. Rev. C 87, 041302(R) (2013).
- [29] G. Roepke, P. Schuck, Y. Funaki, et al., Phys. Rev. C 90, 034304 (2014).
- [30] M. Mirea, arXiv:1411.3152v1 (2014).
- [31] P. Möller and J.R. Nix, Nucl. Phys. A **272** 502 (1995).
- [32] J. Dudek, W. Nazarewicz, and T. Werner, Nucl. Phys. A341, 253 (1980).
- [33] L. Liu, Z.-H. Zhang, P.-W. Zhao, arXiv:1412.5069v1 (2014).